

# PROCEEDINGS OF SPIE

[SPIDigitalLibrary.org/conference-proceedings-of-spie](https://spiedigitallibrary.org/conference-proceedings-of-spie)

## Current status of the facility instruments at the Large Binocular Telescope Observatory

Rothberg, Barry, Power, Jennifer, Kuhn, Olga, Thompson,  
David, Hill, John, et al.

Barry Rothberg, Jennifer Power, Olga Kuhn, David Thompson, John M. Hill, R. Mark Wagner, Christian Veillet, "Current status of the facility instruments at the Large Binocular Telescope Observatory," Proc. SPIE 11447, Ground-based and Airborne Instrumentation for Astronomy VIII, 1144706 (13 December 2020); doi: 10.1117/12.2563352

**SPIE.**

Event: SPIE Astronomical Telescopes + Instrumentation, 2020, Online Only

# Current Status of the Facility Instruments at the Large Binocular Telescope Observatory

Barry Rothberg<sup>a,b</sup>, Jennifer Power<sup>a</sup>, Olga Kuhn<sup>a</sup>, David Thompson<sup>a</sup>, John M. Hill<sup>a</sup>, R. Mark Wagner<sup>a</sup>, and Christian Veillet<sup>a</sup>

<sup>a</sup>Large Binocular Telescope Observatory, 933 North Cherry Avenue, Tucson, AZ 85721, USA

<sup>b</sup>Department of Physics and Astronomy, George Mason University, MS 3F3, 4400 University Drive, Fairfax, VA 22030, USA

## ABSTRACT

Presented here is a review of the status of facility instruments at the Large Binocular Telescope Observatory (LBTO). These include: the prime-focus optical Large Binocular Cameras (LBCs); optical Multi-Object Double Spectrograph (MODS) for imaging and spectroscopy; and the two LBT Utility Camera in the Infrared (LUCIs) for imaging and spectroscopy, which include the commissioning of the Single conjugated adaptive Optics Upgrade for LBT (SOUL). Recently, the Potsdam Echelle Polarimetric and Spectroscopic Instrument (PEPSI), a fiber-fed high resolution optical echelle spectrograph with polarimetry capabilities, has transitioned from a Principal Investigator (PI) instrument to a facility instrument. We discuss the "binocular lifestyle" including the unique challenges of using LBT in three ways: Duplex mode, with identical configurations on both sides (effectively an 11.8 meter mirror); Fraternal Twin (same instruments with different configurations) or Mixed mode, (different instruments on each side) which gives observers two 8.4 meter telescopes to use; or 22.65 meters in interferometry (LBTI) mode. We also review recent changes in nighttime operations at the observatory in response to the COVID-19 pandemic and plans for the implementation of the Health and Instrument Performance plan for the Observatory (HIPO), a program to proactively monitor the health and stability of the facility instruments.

**Keywords:** ELT, Observatories, Instrumentation, Binocular, Spectroscopy, Imaging

## 1. INTRODUCTION

### 1.1 Location and Partnership

The Large Binocular Telescope (LBT) is part of the Mount Graham International Observatory (MGIO), which is located at an elevation of 3,192 meters at Emerald Peak on Mount Graham. LBT shares the site with the 1.8 meter Vatican Advanced Technology Telescope, and the 10-meter Sub-millimeter Telescope. Mount Graham is part of the Pinaleno Mountains located in southeastern Arizona, near the city of Safford. Access to MGIO is restricted from mid-November to mid April and requires the use a four-wheel drive vehicle due to the combination of unpaved roads and winter weather conditions.

The LBT is an international partnership which includes public universities in Arizona (25% share of time) comprising the University of Arizona, Arizona State University and Northern Arizona University; Germany or LBT Beteiligungsgesellschaft (25% share of time), which includes the German institutes of Landessternwarte Königstuhl, Leibniz Institute for Astrophysics Potsdam (AIP), Max-Planck-Institut für Astronomie, Max-Planck-Institut für Extraterrestrische Physik, and Max-Planck-Institut für Radioastronomie. German federal funding requires that some of this time is available to other public universities within Germany; Italy or Istituto Nazionale di Astrofisica (25% share of time) which is responsible for LBTO offering access to the Italian community; the Ohio State University (15.625% share of time); and the University of Notre Dame, University of Minnesota, and University of Virginia (each with 3.125% share of time).

---

Further author information: (Send correspondence to Barry Rothberg)

E-mail: brothberg@lbto.org, Telephone: +1 520 626-8672, Fax: +1 520 626-9333

## 1.2 On-Sky Operatons

### 1.2.1 Standard Operations

Normally, the LBT operates on-sky from September 1-July 10 each year. Between July 11-August 31 the observatory closes for monsoon season in southern Arizona which provides for down-time that is used for telescope and instrument maintenance, upgrades, and one mirror aluminized while the other is washed. Since 2017, and until very recently, the observatory moved to a model where visiting astronomers were encouraged to operate the scientific instruments from a remote observing room at LBT headquarters. These are located in the Steward Observatory building on the campus of the University of Arizona located in Tucson, Arizona. Regardless of whether visiting astronomers operate the instruments from the summit or the Tucson remote observing room, night support for the facility instruments is provided by one of the three staff astronomers. Support is provided either in-person (at the beginning of a science run) or on-call after the first two nights. In late 2019, the Arizona share of LBT time moved to queue operations. LBT service observers execute science programs based on ranked programs matched to current sky conditions. When these programs cannot be executed due to sub-standard sky conditions and/or instrument downtime, programs are executed from a pool of poor weather or backup programs.

### 1.2.2 COVID-19 Operations (C-19 Mode)

In mid-March 2020, the observatory shut down in response to the COVID-19 pandemic. Night operations resumed June 1, 2020, beginning with engineering checks to verify the operational status of all facility instruments. Limited science observations along with Adaptive Optics (AO) commissioning were executed during June and July. The observatory underwent a shorter than standard summer shutdown (July 21 through August 20) with minimal maintenance performed (neither primary mirror was aluminized). LBT returned to on-sky operations for 2020B on August 21 beginning with restart operations and moving to partner science observations in early September. Due to the current limitations on national and international travel, observations are now carried out by LBT staff (either staff astronomers or service observers) on behalf of, and in coordination with the LBT partners. Commissioning of instruments is currently limited. Due to safety concerns, staff astronomers and service observers primarily operate the instruments from off-campus, although several remote observing rooms are available in LBTO HQ in Tucson. Visits to the mountain are restricted. This mode will continue through the end of the 2020B semester, and may continue into 2021A. Plans are underway to develop “satellite” remote facilities among partner institutions. Originally meant as a way to reduce travel costs for partners, this may be implemented in the coming semester to augment C-19 Mode.

In this conference proceeding, we present a summary of the operations and capabilities of the LBT scientific facility instruments that are available for partner science observations. It is an update to the reviews of Rothberg et al. (2016<sup>1</sup> and 2018<sup>2</sup>). Since 2017, LBT has routinely operated in full binocular mode for all facility instruments, including the availability of AO for one or both near-infrared imager & spectrograph.

## 2. THE LARGE BINOCULAR TELESCOPE

### 2.1 Overview

LBT houses two 8.4 meter primary mirrors affixed to a single compact altitude-azimuth mount housed in a co-rotating enclosure. The center-to-center separation between the two mirrors is 14.4 meters. The unique design of LBT allows for its use in three configurations: 1) “Twinned” or Duplex mode in which each mirror has identical instrument configurations yielding an effective collecting area of 11.8 meters; 2) Interferometric mode, which uses the baseline from edge to edge of the two primary mirrors to create an effective aperture of 22.65 meters; and 3) “Heterogeneous” mode, in which each 8.4 meter primary mirror is configured with a different instrument configuration. This could include “fraternal,” in which the same instrument pairs are used, but configured differently (e.g. each LUCI using a different grating or wavelength coverage), or “mixed mode,” in which a different instrument is configured for each mirror (e.g. imaging on one side, spectroscopy on the other). In either case, Heterogeneous mode allows each mirror to operate as two semi-independent telescopes (see 2.3).

The binocular telescope mount includes on each side: four Bent Gregorian focal stations (three of which have space for instrument rotator bearings) accessible via a tertiary mirror, one Direct Gregorian focal station, and two swing arms (one holding a secondary mirror, the other containing a prime focus instrument). All

instruments (whether facility or otherwise) are always mounted on the telescope. The transition time to switch among instruments ranges from 7-10 minutes between the various Gregorian focal stations (including moving a tertiary mirror) and up to 20 minutes to switch from a bent Gregorian station to prime focus (including moving all swing arms). The left-side of the telescope is denoted as *SX* (the 'S' from the Italian word for left, *sinistra*), and the right-side is denoted as *DX* (the 'D' from the Italian word for right, *destra*). Figure 1 shows a layout of the LBT, including locations of all currently installed instruments.

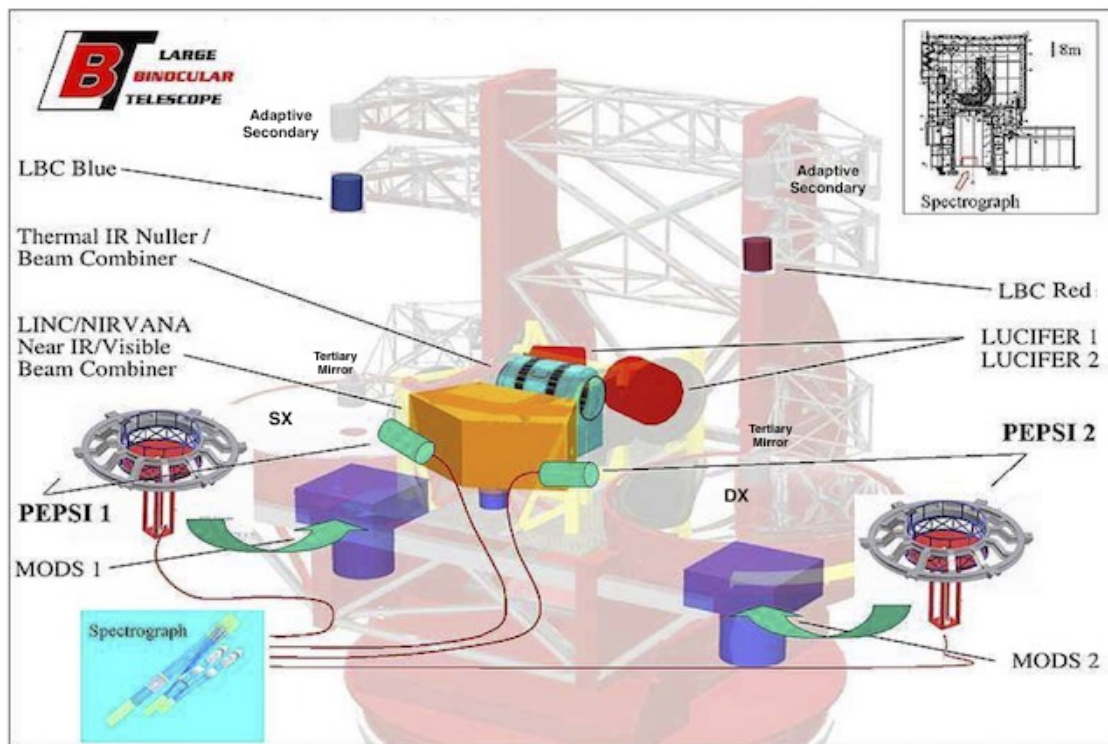


Figure 1: Diagram of the LBT (courtesy of K. Strassmeier). Shown are the locations of the installed instruments, secondary and tertiary mirrors, and an inset diagram with the location of the PEPSI spectrograph.

## 2.2 Types of Instrumentation

There are three categories of LBT scientific instrumentation. The first are *facility instruments*, which are available for use by anyone within the partnerships. Facility instruments are supported and maintained by LBTO personnel. The second type is *Principal Investigator instruments*. These are maintained and operated by the instrument builders, however, they may be used by LBT partners for science on a collaborative basis through time exchanges at the discretion of the PI. LBT staff provide technical assistance primarily limited to interfacing with the telescope control systems and infrastructure. Currently, there are no PI instruments available for use on-sky, although several are planned for future development. The Potsdam Echelle and Polarimetric Spectroscopic Instrument (PEPSI) was formerly a PI Instrument, but is now transitioning to a facility instrument. The third type of LBT instrumentation is *Strategic instruments*. These are defined as technically challenging, designed to push the limits of astronomical instrumentation, and have a major impact on astronomy. Strategic instruments may be available to the LBT community on a collaborative basis or through time exchanges with the PI. Currently there are two such instruments. The first is the LBT Interferometer (LBTI), which can use one or both primary mirrors with LMIRCam (1-5  $\mu\text{m}$ ) for imaging, or one mirror for low-resolution integral field spectroscopy (Hinz et al. 2018<sup>2</sup> and Stone et al. 2018<sup>3</sup>), or Fizeau imaging interferometry; and the NOMIC (8-13  $\mu\text{m}$ ) camera which can be used for aperture imaging, nulling interferometry, and Fizeau imaging interferometry (Leisenring et al. 2012,<sup>4</sup> Hoffmann et al. 2014,<sup>5</sup> and Spalding et al. 2019<sup>6</sup>). It should be noted that while LMIRCam is technically

a facility instrument, it operates within the environment of LBTI, which is a strategic instrument. The second is the LBT INterferometric Camera and the Near-IR/Visible Adaptive iNterferometer for Astronomy (LINC-NIRVANA) a multi-conjugate adaptive optics (MCAO) near-IR imaging system that provides both ground-layer and high-layer corrections (see Herbst et al. 2018<sup>7</sup> and references therein). Further discussion of PI and Strategic instruments are beyond the scope of this paper.

### 2.3 Telescope Movement & Co-Pointing

LBT has been routinely operating as a fully binocular telescope with all of its facility instruments for more than two years. This includes binocular operations not only with pairs of the same instruments, but “mixed mode” operations in which different instrument combinations are used together. Binocular operations require a very different approach to observing. One must consider both the advantages and limitations of two semi-independent mirrors on a fixed mount. The telescope control system (TCS) accepts and processes requests from the science instruments to move to a target on sky (called a “preset”). When the telescope is configured for binocular operations, the TCS expects a preset from the SX and DX sides of the telescope. If only one preset is sent, the telescope will not move. The telescope mount points near the mid-point between the two sides and the telescope software “knows” to avoid offsets that would violate the “co-pointing limit.” This limit is defined as the maximum physical travel distance allowed between the two mirrors. The Pointing Control Subsystem (PCS) decides and resolves requests to move the mount or the mirrors as needed. The software imposes its own co-pointing limit, currently, it is  $\sim 40''$  in radius. This is smaller than the physical limit and will throw an error and not move the mirrors if a request is made that violates this limit. The actual limit on sky varies because it is also affected by the movement and the position of the secondary and tertiary mirrors. The facility instruments are currently operated so that scripts will only allow binocular observations which have the same field center and same position angle (PA) on-sky. This is not a hardware or TCS limitation, but an operational restriction. In some cases this is due in part to how the instrument sends presets to the TCS, but also takes into account the difficulty in planning observations that may more readily violate the co-pointing limits. This would require more sophisticated planning software to take all the variables into account to avoid such pitfalls. However, the telescope was designed to allow a preset to have different field centers and PAs, as long as they do not violate the co-pointing limits. When both sides of the telescope are pointing at the same position on the sky, the co-pointing limit will not be violated (See Figure 2). However, once the mount completes a preset, each side may operate independently. For example, this may occur if one side is used for spectroscopy and the other is used for imaging.

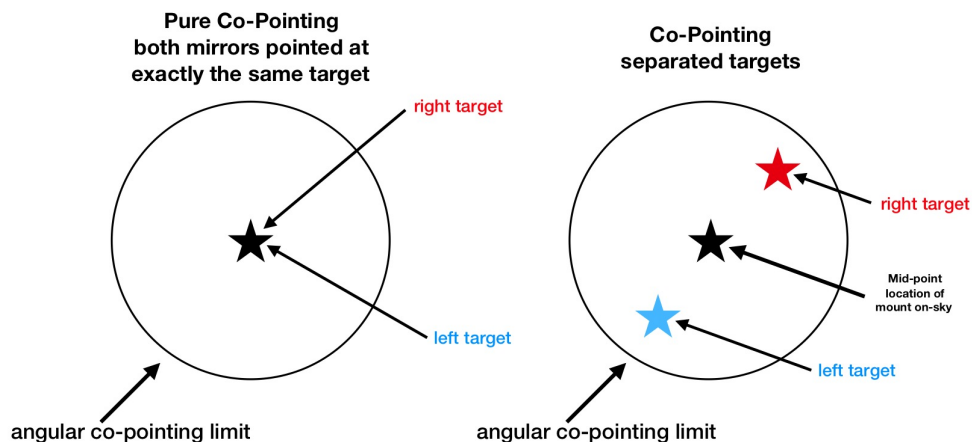


Figure 2: Left - Diagram of “pure co-pointing” (same target both sides); Right - co-pointing with different targets.

There are two types of motions, “synchronous” or “asynchronous.” Synchronous motion assumes that both sides of the telescope move at the same time. In cases where the SX and DX side need to move a distance greater than the co-pointing limit (e.g. a blind offset or dithering), the command to move must be synchronous. However, synchronous presets can also be sent for small movements that do not approach the co-pointing limits (e.g. aligning science targets in a spectroscopic slit). Some instruments are set up to send synchronous presets regardless of whether or not large moves are needed. Asynchronous movement occurs in cases where the SX and DX sides move independently. Asynchronous *presets* can be made in cases where one side of the telescope encounters a problem or other failure after a new preset. A second asynchronous preset can be sent on the side with problem so as not to interfere with observations already occurring on the other side of the telescope. Asynchronous movements are executed one at a time by the TCS as long as they do not violate the co-pointing limits. For more details see De La Peña et al. (2010).<sup>8</sup>

LBT may also be configured for monocular operations (i.e. single sided operations), in which case the TCS expects a preset from only the authorized side of the telescope. This is used when only one instrument in a pair is available. A hybrid configuration also exists called “pseudo-monocular” mode, in which only one side of the telescope is authorized to move the mount, but once on target, both sides may send commands to move their respective mirrors. This mode is needed for some combinations of mixed mode operations.

### 3. FACILITY INSTRUMENTS

#### 3.1 Large Binocular Cameras (LBCs)

##### 3.1.1 Instrument Layout

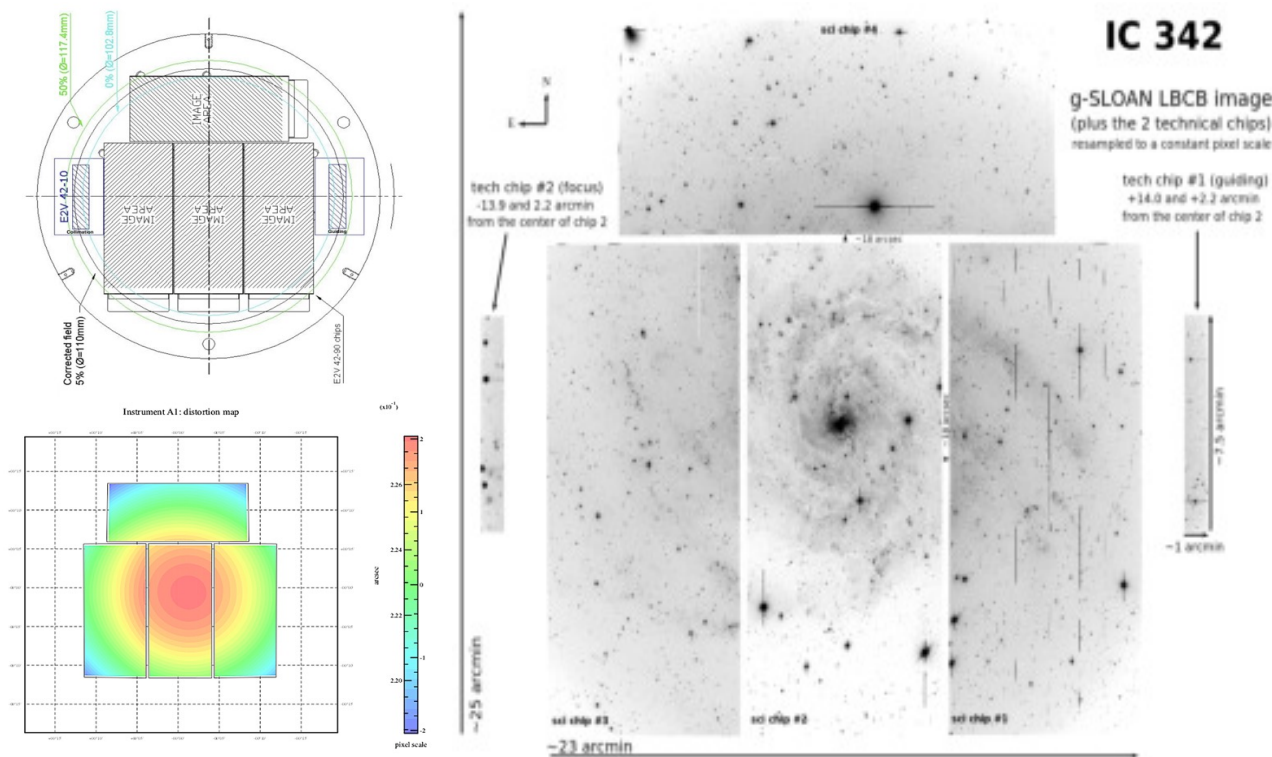


Figure 3: Top Left - the chip layout of LBC Blue (the four science chips and the two technical chips used for collimation and guiding); Bottom left - a distortion map of LBC-Blue; Right - 3600 sec *g*-sloan image of the galaxy IC 342 (observed by B. Rothberg and processed by O. Kuhn to remove the distortions and re-sampled to a constant scale of  $0''.224 \text{ pixel}^{-1}$ ).

The Large Binocular Cameras (LBCs) are comprised of two wide-field  $f/1.14$  imagers, one optimized for blue wavelengths ( $0.33\text{-}0.67\mu\text{m}$ ), the other optimized for red wavelengths ( $0.55\text{-}1.11\mu\text{m}$ ). Each LBC operates at the prime focus location of their respective mirrors (LBC-Blue at SX and LBC-Red at DX). They are each mounted on a spider swing-arm that can be deployed above the primary mirror and moved into and out of the telescope beam as required. The LBCs were accepted as facility instruments in October 2011 and were the first instruments to make full use of binocular observing at LBT. When used in a binocular configuration the LBCs dither simultaneously using the mount, rather than each mirror moving independently. The advantages are quicker movement on sky and no need to worry about violating the co-pointing limits. The disadvantage is that with slightly different readout times and filter motions between the two cameras, as well as variations in the exposure times needed between blue and red filters, one side of the telescope can potentially sit idle while the other continues to collect photons before the mount offsets to a new position on sky.

The LBCs each contain six E2V CCD detectors, four of which are used for science. The four science CCDs are each  $2048 \times 4608$  ( $13.5\mu\text{m}$  square pixels) and are arranged in a mosaic with three abutted next to each other. A fourth CCD is rotated clockwise 90 degrees and centered along the top of the three science CCDs (see Figure 3). Each CCD covers  $7'.8 \times 17'.6$  with a gap of 70 pixels ( $18''$ ) between each CCD. This yields a  $23' \times 25'$  field of view (FOV). In order to obtain an uninterrupted image, dithering is required to fill the gaps between CCDs (and recommended to correct for cosmic rays and bad pixel columns). The other two CCDs are  $512 \times 2048$  ( $13.5\mu\text{m}$  square) pixel CCDs and do not have shutters. They are placed on either of the science CCD chips. One is within the focal plane and is used for guiding adjustments, the other is out of the focal plane and uses extra-focal pupil images to maintain collimation and focus. Figure 3 shows the layout of LBC-Blue (similar to LBC-Red) corrected field size, and an example of a  $g$ -sloan image.

Each of the LBCs house two filter wheels, each with 5 slots. Currently, LBC-Blue contains only six filters, these are listed in Figure 4 along with their transmission curve. There are currently ten filters available for science for LBC-Red, although only eight can be used on sky at any given time. The two extra filters are TiO 784 and CN 817 which were purchased and tested in semester 2014B by Landessternwarte Königstuhl (LBTB-Germany).

### 3.1.2 Improvements to Collimation and Image Quality

LBC collimation is particularly sensitive to temperature differences between the ambient temperature in the enclosure and the mirror glass which leads to large aberrations, particularly at the start of the night. Originally, collimation was done using the IDL based Focal Plane Image Analysis (FPIA) task which measures and analyzes highly de-focused images of stars (pupils). See Hill et al. (2008)<sup>9</sup> for more details. Zernike corrections (Z4, Z5, Z6, Z6, Z8, Z11, and Z22) are computed and applied to remove the aberrations. A small region of Chip 2 just below the rotator center on each LBC is read out in order to speed up the process. The process is repeated until the corrections converge. However, this requires a field with a sufficient number of bright stars. If there are too few stars and/or they are faint, then the algorithm has trouble properly measuring the pupils and determining the appropriate corrections.

The next step in improving collimation, the Wavefront Reconstruction Software (WRS) was developed by Stangalini et al. 2014.<sup>10</sup> It selects the brightest pupils in a field to measure but only if it meets a certain threshold for signal-to-noise (S/N). WRS analyzes the moments of the intensity distribution of the pupils and from that reconstructs a model of the pupil. WRS provides the biggest improvements when significant coma is present at the start of the night (Z7 and/or Z8) and/or there exists significant temperature gradients which can lead to spherical aberrations (Z11 or Z22). Due to the amount of time it takes for WRS to converge it is now run in combination with FPIA at the start of a night (or when the LBCs are first used during the night). This combination package first runs WRS to deal with coma and spherical aberrations, then continues to collimate with FPIA. After this, the original FPIA is run every 30 minutes to maintain collimation or after large slews across the sky to a new target.

LBT is currently testing an improved method of collimation using telescope metrology (ultra-high accuracy measurements of the mirrors), called the Telescope Metrology System (TMS). This method uses a multi-channel absolute distance measuring fiber-interferometer system which can measure the motions and vibrations of objects with an accuracy of a few tenths of a micron (Rakich et al. 2018<sup>11</sup>). A prototype of the system was installed during 2017 and was able to measure the semi-absolute distance between the primary mirror and prime focus corrector to a level of  $1\mu\text{m}$  *r.m.s.*. Part of the TMS project includes modeling of the optical elements of both

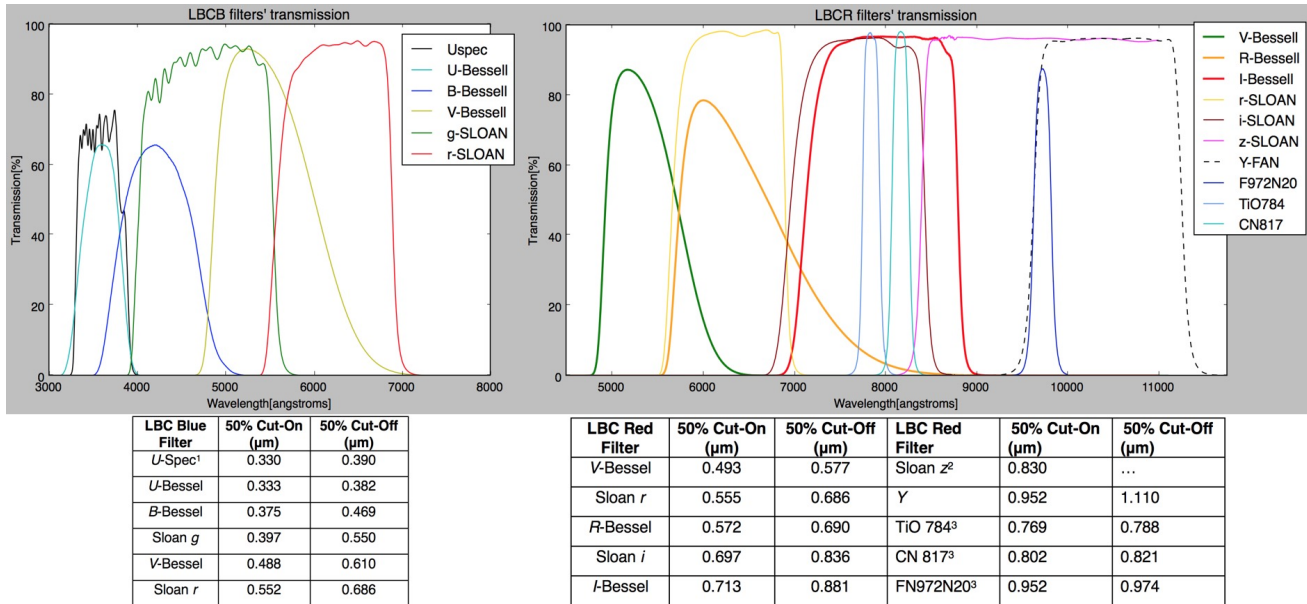


Figure 4: Left - A plot of the transmission curves for the LBC-Blue filters. Right - A plot of the transmission curves for the LBC-Red filters. Below each plot is a table of filters for each LBC. <sup>1</sup>Broad width (top-hat) filter response designed to mimic the spectroscopic coverage in this wavelength range. The filter has a bandpass that depends on angle of incidence, with a 10-15 angstrom blueshift from normal to 26° angle of incidence. Filter transmission scans obtained in the summer of 2016 by the NOAO spectrometer show some non-uniformity across the filter. <sup>2</sup>The *z*-sloan filter has no red cutoff and is limited only by the detector quantum efficiency ( $\simeq 0$  at  $1.1\mu\text{m}$ ). <sup>3</sup>Medium width filters

LBCs. Combined with a modeling of the LBT's prime focus, this is used to predict what the image quality should be and to determine if any elements of the optical system may be misaligned. There are known issues with the image quality of both LBCs that have yet to be solved and this work should help constrain and improve these issues.

Recently, TMS been used in passive mode on the DX side with LBC-Red. The system collects telemetry with the goal of comparing the collimation that would have been calculated with those actually computed by FPIA and WRS. Just recently, TMS was used in active mode to compute and apply collimation updates to LBC-Red. These tests will continue during upcoming engineering nights. The goal is to account for all motions between the LBCs and primary mirrors and be able to collimate without interrupting science observations and moving the telescope to a collimation field. The tests are part of a collaboration between the Giant Magellan Telescope Organization and LBT. The next steps for TMS testing include installation and active collimation for LBC-Blue and expending the system to the Gregorian Foci. However, the laser system operates at  $1.53\mu\text{m}$ , which has been shown to impact LUCI operations. For more information see Rodriguez et al. 2020<sup>12</sup> and Rakich et al. 2020 (Paper 11445-21, this conference).

### 3.1.3 Example of the Power of the LBCs

The sheer light collecting power and wide-field coverage of the LBCs make them formidable instruments for not only large surveys of the most distant objects, but for tracking fast moving objects in our Solar System. In 2017, the LBCs were the first terrestrial instruments to detect the OSIRIS-REx spacecraft on its slingshot around Earth. The detection was made two weeks before any other observatory (Rothberg et al. 2018<sup>2</sup>). Recently, the LBCs were used to make the first multi-wavelength follow-up observations of 2020SO, a near-Earth object identified by the Pan-STARRS survey. By observing the object with several filters, color information was used to constrain the composition of the object. Based on these, and subsequent observations to refine the orbits, it

was determined the object is most likely the spent upper stage of a Centaur rocket used to launch Surveyor-2 on September 20, 1966.

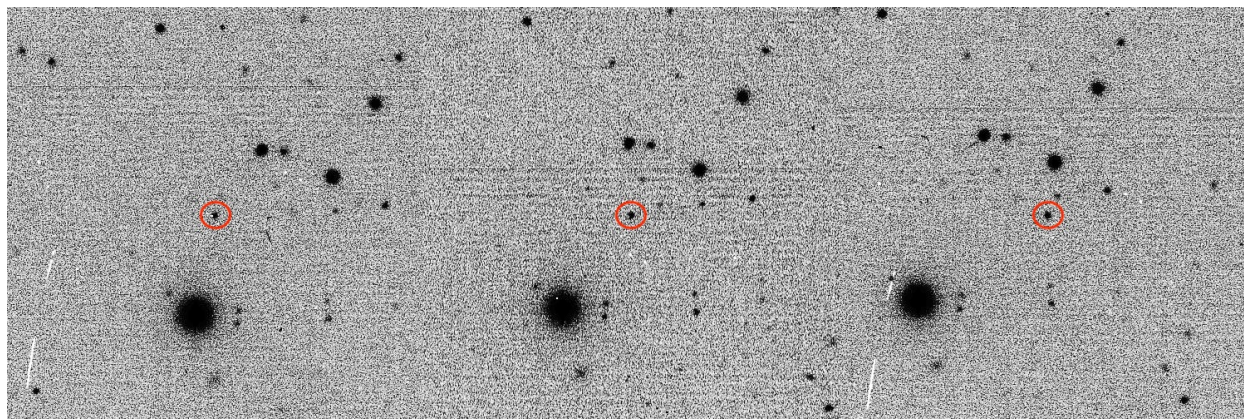


Figure 5: LBC-R *i*-sloan images from September 28, 2020 tracking 2020SO. This object was thought to be a new “mini”-Moon, but based on multi-wavelength observations first obtained with the LBCs on LBT, and later confirmed by other observatories, it is now thought to be the spent stage of a Centaur rocket launched in the 1960s. Astrometry and processing by C. Veillet.

## 3.2 Multi-Object Double Spectrograph (MODS)

### 3.2.1 Instrument Layout

The Multi-Object Double Spectrographs (MODS) are a pair of identical instruments, each capable of imaging, or spectroscopy using longslit and user-designed multi-object slit (MOS) masks. Each MODS is mounted at the direct Gregorian  $f/15$  port (MODS-1 on SX and MODS-2 on DX, see Figure 1). The MODS were designed and built by The Ohio State University as part of its contribution to the first generation of LBT instruments. Specific details can be found in Pogge et al. (2012)<sup>13</sup> (and references therein). MODS-1 was installed in 2009 and became available for partner science in 2011B. MODS-2 was installed in early 2014 and commissioned from 2014-2015. Both MODS have been used for science on-sky in some capacity since late 2015.

MODS has two observing modes: direct imaging; and spectroscopy using curved focal plane masks. The optical layout of MODS incorporates a dichroic beam splitter below the focal plane that splits light into separate, but optimized blue and red only channels. There is a cross-over at  $0.565 \mu\text{m}$  that results in a drop in flux in a small region ( $\sim 0.005 \mu\text{m}$  centered on this wavelength). For some science cases, users may choose to employ blue- or red-only observations. The dichroic is replaced with no optic in the beam for blue-only mode and replaced with a flat mirror for red-only mode (imaging and spectroscopy). Direct imaging is achieved by replacing the grating with a plane mirror and is used for target acquisition for spectroscopy. The standard longslit spectroscopic acquisition is to read out a smaller  $1\text{K} \times 1\text{K}$  region of the CCD to reduce overheads. MODS includes a full complement of sloan filters:  $u$ , and  $g$  for the Blue channel; and  $r$ ,  $i$ , and  $z$  for the Red channel. The usable FOV is  $6' \times 6'$  but with degraded image quality at radii  $> 4.5'$ . In the case of direct imaging for science, the CCDs are read out in  $3\text{K} \times 3\text{K}$  mode.

MODS has two spectroscopic modes: a medium resolution diffraction grating optimized for blue and red spectral regions with  $R \sim 2300$ , and  $1850$  (assuming a  $0''.6$  wide slit and scaling with slitwidth), respectively. The grating dispersion uses the full full  $8\text{K} \times 3\text{K}$  CCD, and regardless of where slits are placed in the  $6' \times 6'$  the full wavelength range is dispersed across the CCD; the second spectroscopic mode uses a prism which produces a low-dispersion spectroscopic mode with  $R \sim 420-140$  in the blue, and  $R \sim 500-200$  in the red and uses a  $4\text{k} \times 3\text{K}$  readout mode. Longslit and multi-object slit masks are made available through a mask cassette system with 24 positions. Each mask is matched to the shape of the Gregorian focal plane. The first 12 positions in the cassette contain permanent facility and testing masks. The facility science masks include:  $0''.3$ ,  $0''.6$ ,  $0''.8$ ,  $1''.0$ ,  $1''.2$ , and  $2''.4 \times$  longslit segmented masks (each contains five  $1'$  long slits each separated by  $3''$  segmented

braces); a 5'' wide  $\times$  60'' longslit single segment mask used primarily for spectro-photometric calibrations; and a pointing mask which can be used to block bright nearby targets in imaging more. The remaining 12 mask slots are available for custom designed MOS masks (see 3.5). The MODS MOS and facility masks are housed in a cassette system and accessed much in the same way as a music jukebox. It is located within the MODS housing and accessed through a panel on the side of the instrument. Custom mask exchanges take place on the first day of a partner science block. If needed, MODS MOS masks can be exchanged with new masks during the night.

The acquisition, auto-guiding and wavefront-sensing systems (AGW) are a part of MODS and located above the instrument focal plane, but within the unit itself. The AGW patrol field is 5'  $\times$  5' and overlaps with the bottom half of the MODS science field. The guideprobe can potentially shadow the science field or science mask if a guidestar is not chosen carefully. MODS uses an infrared laser ( $\lambda = 1.55 \mu\text{m}$ ) closed-loop image compensation system (IMCS) to provide flexure compensation due to gravity, mechanical, and temperature effects (Marshall et al. (2006)<sup>14</sup>). MODS also houses continuum and arc lamps internally for calibration.

Binocular observations with MODS-1 & MODS-2 have become routine for nighttime operations since mid-fall of 2016. The filters, gratings, facility longslits, and overall efficiency of MODS-1 & MODS-2 were designed to be virtually identical. Observations with the same instrument configuration used for both MODS is effectively a single MODS observation obtained with an 11.8 meter diameter mirror. To date, the only known mechanical variation between the two MODS are the intensity of the internal lamps used for calibrations (flats and arcs). However, in the last two years there is evidence that the sensitivity of MODS-1 (and possibly relating to the SX telescope) is lower than that of MODS-2\*. Currently, MODS-Binocular observations can be run in either duplex mode, where the observing script is "twinned" and the same instrument configuration is used with both MODS (i.e. same imaging filters, or same longslit mask and grating, or same MOS mask), or "fraternal twin" mode, where each MODS uses a different MOS mask, or a combination of imaging on one side and spectroscopy on the other. The only constraint is that each MODS must use the same PA and same pointing center. These restrictions are operational only and are designed to avoid violating the co-pointing limit during observations. Figure 6 shows an example of recent observations of a Gamma Ray Burst target (GRB200826A or AT2020scz) in which observations from both sides were combined in order to detect a faint object.

### 3.3 LBT NIR Spectroscopic Utility with Camera Instruments (LUCI)

#### 3.3.1 Instrument Configuration

The two LBT Utility Camera in the Infrared instruments (LUCI, formerly LUCIFER), are a pair of cryogenic near-Infrared (NIR) instruments, with imaging and spectroscopic (longslit and MOS) capabilities. LUCI-1 is mounted at one of the  $f/15$  Bent Gregorian focus on the SX side and LUCI-2 is similarly mounted on the DX side (see Figure 1). The LUCIs can operate at wavelengths from 0.89  $\mu\text{m}$  (LUCI-1) or 0.95  $\mu\text{m}$  (LUCI-2) through 2.4  $\mu\text{m}$  in one of three modes: seeing limited (SL), Enhanced Seeing Mode (ESM) AO, or diffraction limited AO. Unlike MODS, the guiding and wave-front sensing in seeing limited modes (and initial collimation in ESM and AO modes) are done using external AGW units. The LUCI calibration units are external to the instruments, residing on mounts located above the LUCIs that swing in front of the entrance windows when needed. Additional information regarding design, construction, can be found in Seifert et al. (2003).<sup>18</sup>

LUCI-1 was installed at LBT in September 2008 and LUCI-2 was installed in July 2013. Both are now equipped with 2K  $\times$  2K Hawaii 2RG detectors and have the same set of cameras: an  $f/1.8$  (N1.8) camera which delivers a 0''.25 pixel<sup>-1</sup> plate scale; an  $f/3.75$  (N3.85) camera with a 0''.12 pixel<sup>-1</sup> plate scale; and an  $f/30$  (N30) camera with a 0''.015 pixel<sup>-1</sup> plate scale. The N1.8 camera is primarily used for seeing-limited spectroscopy; the N3.75 camera is used for seeing-limited imaging and delivers  $\sim 4' \times 4'$  FOV. The N3.75 camera can also be used for spectroscopy with 2 $\times$  better resolution and half the wavelength coverage achieved with the N1.8 camera. The N30 camera is used for AO imaging with both LUCIs, delivering a 30''  $\times$  30'' FOV. The N30 camera in LUCI-2 can also be used for diffraction limited spectroscopy due to the presence of a diffraction limited grating (which is not installed in LUCI-1). Both LUCIs also house the same complement of broad, medium, and narrow-band filters (Figure 7 shows the transmission curves for each of the filters). In addition to the filters plotted in Figure 7, both LUCIs have two broad blocking filters used with the low-resolution grating: zJSpec, which covers 0.905-1.31 $\mu$ ; and HKSpec, which covers 1.45-2.44 $\mu\text{m}$ . In the summer and fall of 2019 two neutral density (ND) also

\*<https://sites.google.com/a/lbto.org/mods/sensitivity>

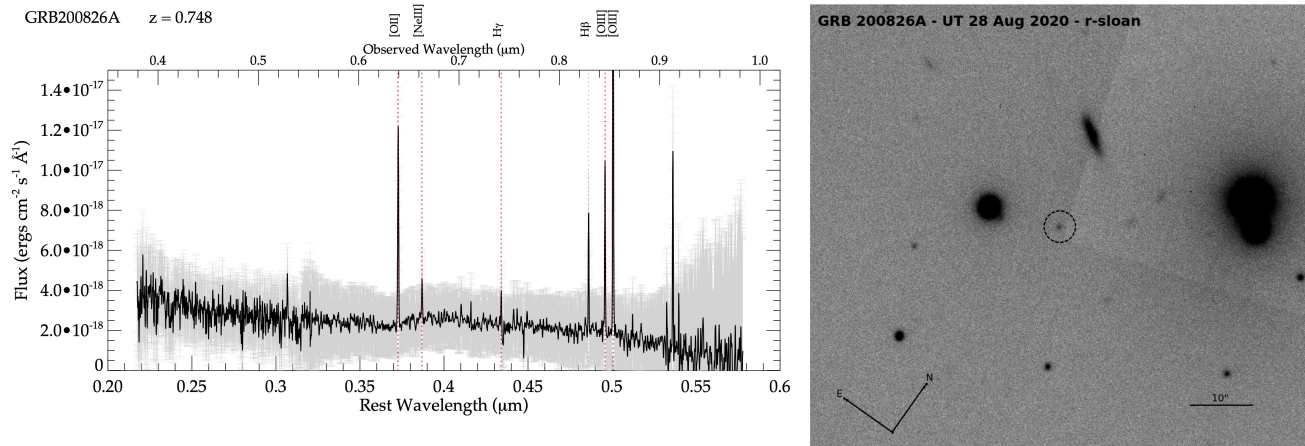


Figure 6: Left - Flux-calibrated binocular MODS spectra of GRB 200826A obtained on UT 28 August 2020. The observations consist of 4 exposures of 900 seconds each in three of the four available channels (MODS-1 Red, MODS-2 Blue, and MODS-2 Red). The channels were combined without shifts or scaling. A  $1''$  wide slit was used ( $R \sim 1200$ ). The spectrum was used to determine the first redshift ( $z = 0.7481 \pm 0.0003$ ) of the host galaxy + GRB using the 5 emission lines over-plotted in the figure. The line at  $\lambda \sim 0.54 \mu\text{m}$  was determined to be noise from poorly subtracted nightsky lines. The grey over-plotted points represent the error spectrum. The spectrum of the underlying host galaxy shows clear evidence of the Balmer break at  $0.4 \mu\text{m}$ . This suggests at least a post-starburst (few Gyr) age to the stellar population of the underlying host galaxy. Right - 60 second acquisition image in r-sloan used for the observations. The AB magnitude of the target is  $r = 22.15 \pm 0.07$ . The observations were reported in Rothberg et al. 2020.<sup>15</sup> Subsequent observations using MODS imaging have been undertaken in collaboration with astronomers from the INAF partnership (Rossi et al 2020<sup>16</sup>). The event appears to be consistent with being a long/soft event (Svinkin et al. 2020<sup>17</sup>).

known as optical density (OD) filters were added to each LUCI: An ND-2 with 1% transmittance, and an ND-4 with a 0.01% transmittance. These two filters were installed primarily to allow for AO engineering observations of bright stars. In LUCI-1, both filters produce a ghost image of bright sources that varies with telescope pointing, while no such ghost is seen in LUCI-2. This suggests something is reflecting the incoming light, either in the filter or near the detector. Until this is corrected, the ND filters in LUCI-1 remain for engineering work, while the ND filters in LUCI-2 can be used for scientific observations. Since 2017A LUCI-1 and LUCI-2 have been released for binocular observations. Currently, the LUCIs can be configured in “twinned mode” (same pointing center, PA, and configuration on both sides) or “fraternal twin” mode (same pointing center and PA, but allows for a mixture of configurations).

There are differences between the available spectroscopic gratings for the two LUCIs. Unlike MODS, where the grating tilt is not changeable by the user, the LUCIs offer a wide range of configuration possibilities that can be achieved with various tilts (i.e. central wavelengths or  $\lambda_c$ ), gratings, slits, and cameras. Using the N1.8 camera, low resolution grating (G200) permits nearly complete coverage of the near-IR window with only two settings. The high resolution grating (G210) with the N1.8 camera allows for nearly full wavelength coverage of each filter (i.e.  $z$ ,  $J$ ,  $H$ , and  $K$ -band). Users also have the flexibility to combine cameras, gratings, slits, and  $\lambda_c$  in different ways to achieve a wide range of scientific goals (i.e. higher spectral resolutions over shorter wavelength ranges). Table 1 lists an overview of the LUCI gratings available. Only LUCI-2 contains an AO quality (diffraction limited) grating (G040). Using the  $0''.13$  longslit, this grating would yield a resolution of  $R \simeq 8000$  and requires two settings to cover a single band-pass. The G040 suffered from significant instabilities during early LUCI-2 commissioning. The grating was repaired during the summer of 2019. However, AO spectroscopy requires additional software updates and testing before it can be released for use (see 3.3.3).

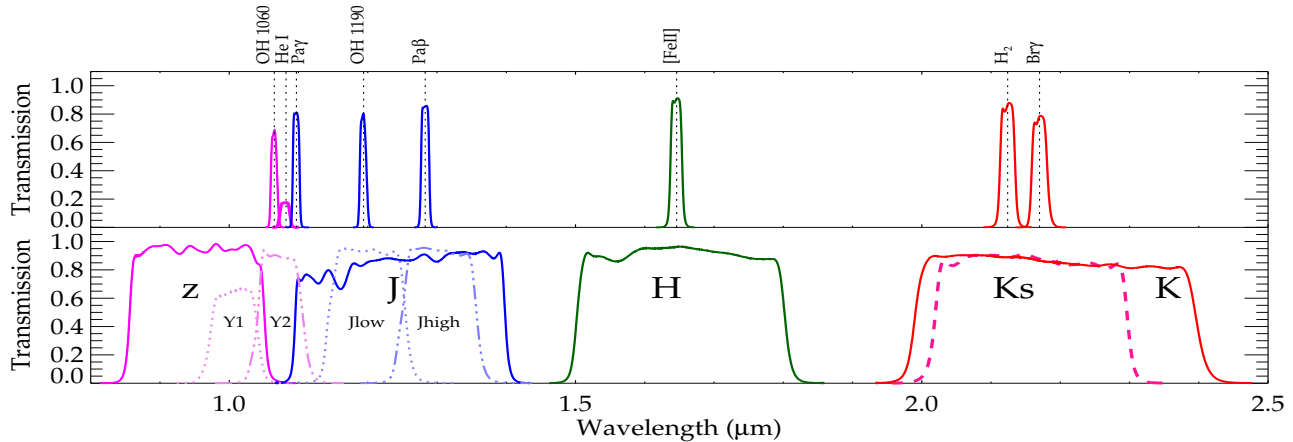


Figure 7: Plotted above are the transmission profiles of the narrow band filter (top panel). The bottom panel shows the transmission curves of the broad-band (z, J, H, Ks, and K) and medium-band (Y1, Y2, J-low, and J-high) filters. The broad-band filters were manufactured by Barr. There is a slight difference between the bandpass and transmission efficiencies of the Barr filters in LUCI-1 and LUCI-2. The LUCI-1 filters are plotted above.

### 3.3.2 LUCI Masks

LUCI-1 and LUCI-2 each use a cryogenic MOS unit to house a set of 10 permanent facility longslit masks ranging in width from  $0''.13$  (AO-only) to  $2''$  as well as an N30 fieldstop mask (to block stray light) for AO observations, a blind mask (for taking dark frame exposures) and optic and spectral sieve masks. A second cabinet can be inserted into each LUCI holding up to 23 user designed MOS slit masks (see 3.5). The MOS unit houses the focal plane unit (FPU) which places the masks in and out of the LUCI focal plane using a robotic grabber arm. The grabber can then rotate almost 180 degrees and slide along a set of rails to the slot containing the requested mask or the empty slot to put back the mask no longer needed (Buschkamp et al. 2010<sup>19</sup>).

LUCI MOS mask exchanges for user designed masks are more time-consuming and complicated than those for MODS, and as a result occur less frequently (only 3-4 times per semester as compared to a dozen or more for MODS). Since the MOS masks are housed internally, they must be cooled to cryogenic temperatures before an exchange. An exchange requires two auxiliary cryostats. One contains the cabinet holding new MOS masks, and a second, empty aux cryo, is used to extract the cabinet currently inside a LUCI. The time from cool-down of the aux cryos for the first exchange until the insertion of the final cabinet in the second LUCI can take approximately six days. The exchanges take place on the telescope infrastructure and requires the aux cryos to be lifted up through a hatch in the floor of the telescope enclosure, and flown up and over the telescope itself. Since the number of exchanges are limited each semester, each LBTO partner is assigned a fraction of the available slots in each cabinet based on the number of nights assigned to them during the block of time covered by an exchange.

### 3.3.3 Flexure

Unlike MODS, flexure compensation is currently passive mode only. The algorithm was updated a few years ago. The corrections are applied to the last fold mirror in the optical train (FM4), which lies in front of the instrument's internal pupil. The corrections come from a pre-populated look-up table of motor values measured from closed dome observations taken at four different elevations and every 10 degrees of rotation. The algorithm reads the current telescope elevation and instrument rotator angles and does a bi-linear interpolation between calibration points and updates the FM4 position on 20 second intervals. These corrections work fairly well for seeing limited observations and modest spectroscopic integration times. However, with the finer plate scale of the N30 AO camera these small shifts span many more pixels. Recent analysis has demonstrated that for imaging, passive flexure works well for a single frame of up to  $\simeq 70$  seconds exposure time. Beyond this, the smearing of the passive flexure counteracts the improvements gained from AO. For background limited observations with the broad-band filters, passive flexure is adequate for AO imaging. However, for narrow-band filters, background

Table 1. Overview of Installed LUCI-1 &amp; LUCI-2 Gratings

| Grating           | Band                 | $\lambda$ -Range ( $\mu\text{m}$ ) | Spectral Width( $\Delta\mu\text{m}$ ) | Resolution <sup>a</sup> |
|-------------------|----------------------|------------------------------------|---------------------------------------|-------------------------|
| G210              | <i>z</i>             | 0.85-1.02 <sup>b</sup>             | 0.124                                 | 5400                    |
| G210              | <i>J</i>             | 1.15-1.35                          | 0.150                                 | 5800                    |
| G210              | <i>H</i>             | 1.50-1.75                          | 0.202                                 | 5900                    |
| G210              | <i>K</i>             | 2.06-2.40                          | 0.328                                 | 5000                    |
| G200              | <i>zJ</i>            | 0.90-1.25 <sup>a</sup>             | 0.440                                 | 2100-2400               |
| G200              | <i>HK</i>            | 1.40-2.40                          | 0.880                                 | 1900-2600               |
| G150 <sup>c</sup> | <i>K<sub>s</sub></i> | 1.95-2.40                          | 0.533                                 | 4150                    |

<sup>a</sup>Spectral Resolution is for the  $0''.5$  slit with the N1.8 camera. The spectral resolution scales with slitwidth and camera scale. <sup>b</sup>Note that the dichroic at the entrance window to each LUCI affects the *z*-band transmission. The dichroic on LUCI-1 cuts off at  $\lambda = 0.85 \mu\text{m}$  and cuts off at  $\lambda = 0.95 \mu\text{m}$  on LUCI-2; <sup>c</sup>Available on LUCI-1 only; Resolution scales with slitwidth. If using the N3.75 camera multiply  $\Delta\lambda$  by 0.48, and if using the N30 camera multiple by 0.06.

limited observations would be negatively impacted by passive flexure.

An active flexure compensation (AFC) system has been developed for use with both diffraction- and seeing-limited observations. In the case of AO observations, this would allow background limited narrow-band imaging observations. AFC is critical for spectroscopic observations of all but the very brightest targets. But its impact is not limited to AO observations alone. AFC significantly improves the subtraction of sky emission lines for spectroscopic observations. The AFC algorithm was developed by Pramskiy et al. 2018<sup>20</sup> and has been tested using closed dome and on-sky observations. The algorithm requires a specific readout mode of the LUCI detector along with the presence of alignment holes in the focal plane. The latter are achieved using spectroscopic masks (longslit). For imaging, these holes are now included as part of the field-stop mask for the N30 camera, which is used to block scattered light. All facility masks have been upgraded to include these alignment holes. In addition, the software which is used to by observers to design multi object spectroscopic masks has been updated to accommodate AFC functionality in future mask designs.

### 3.3.4 LUCI Updates

In addition to AFC, two additional modes are beginning development for LUCI operations. The first is Angular Differential Imaging (ADI). It is a high contrast imaging technique primarily used with AO to remove speckle noise and detect faint companions. The mode works by turning off the instrument rotator (which would normally maintain a fixed PA) and allowing the field of view to rotate. The highest contrast is gained by observing a target during its transit time across the meridian. The capability has been tested on-sky successfully using AO but is not officially offered because it requires manual editing of the LUCI XML scripts. Updates to the observing tool will allow users to plan and generate scripts that support ADI in the same manner as other observations. The second update is the ability to read out a sub-frame of the LUCI detector. The capability currently exists in the software which directly interfaces with the LUCI detectors, and is routinely used during AO commissioning observations of bright stars, and has been used during recent science commissioning time. Sub-frame readout currently requires manual intervention to “acquire” the target and configure the software to read out the detector around the target. This mode is critical bright-target AO observations to avoid saturating the detector ( $K \leq 11.5$  mag will saturate using the shortest readout time of 2.51 seconds). The upgrade will allow sub-frame readout and acquisition with the LUCI software, and planning and generating of scripts using the observing tool.

## 3.4 LUCI & MODS Together on the Frontier of Science

Shown in Figure 8 is a color image from the Sloan Digital Sky Survey (center), optical spectra from MODS (left), and near-infrared spectra from LUCI (right) of the galaxy SDSS J084905.51+111447.2. This target was part of a sample of interacting galaxies suspected of hosting two active galactic nuclei (AGN). Targets were selected based on evidence of galaxy interactions, and X-ray and thermal infrared emission consistent with at

least one AGN. The three bright points were found to be galaxy nuclei, implying a triple merger! Near-IR spectra obtained from LUCI-2 showed evidence of AGN activity in Galaxy 1 and Galaxy 3, but not Galaxy 2. Binocular MODS observations were then obtained of the nuclei of Galaxy 1 and Galaxy 2 to look for further evidence of an AGN. From the synergy among LUCI spectra, MODS spectra, space-based Chandra and NuStar X-ray observations, and thermal infrared emission from the space-based Wide-field Infrared Survey Explorer (WISE), SDSS J084905.51+111447.2 became the first confirmed *triple* AGN system discovered. Taken separately, none of the observations alone could have confirmed the existence of three AGN in this ongoing merger.

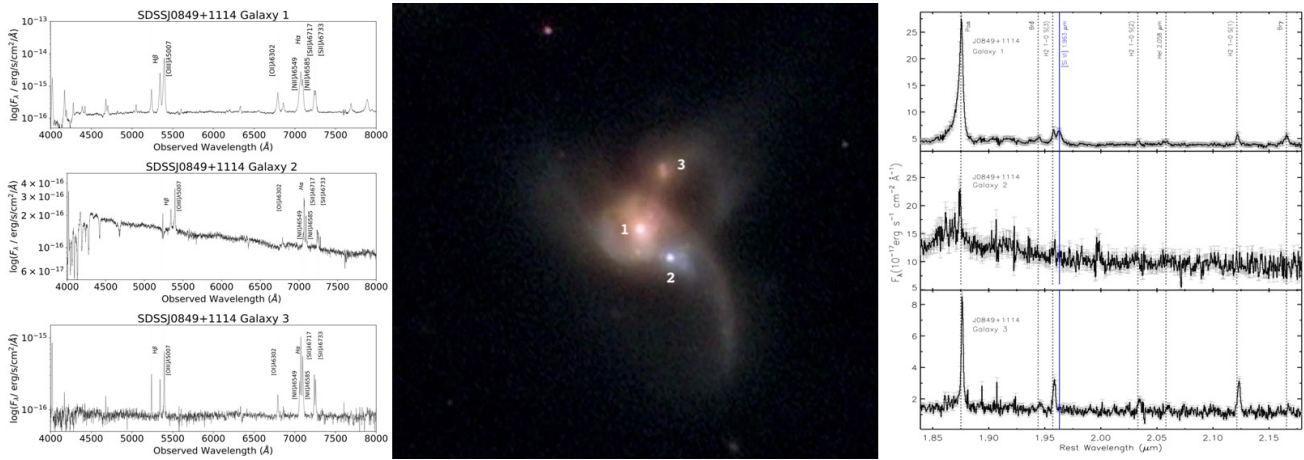


Figure 8: The Triple AGN Merger SDSS J084905.51+111447.2. The system is comprised of three galaxies, each hosting an AGN. Shown above are the optical spectra for the nuclei of each galaxy (left), two of which were obtained from MODS (Galaxy 1 and Galaxy 2); a color image of the galaxy constructed from SDSS imaging (center); and near-IR spectra obtained from LUCI-2 for each nucleus. The location of each nucleus is marked in the color image. The results were presented in Pfeifle et al. 2019.<sup>21</sup>

### 3.5 Designing and Using Multi-Object Spectroscopic (MOS) Masks

A unique capability among the spectroscopic facility instruments (MODS and LUCI) is the capability to use multi-object spectroscopic (MOS) masks designed by users. These masks allow the placement of multiple slits, including straight, angled, and curved, in the focal plane. Combined with a binocular telescope, this increases MOS efficiency by either reducing the amount of time on-sky needed to collect photons, or to cover twice as much real-estate on-sky.

MODS and LUCI MOS masks are designed using similar software, the Lucifer Mask Simulator (LMS) for LUCI and the MODS Mask Simulator (MMS) for MODS. MMS and LMS use the European Southern Observatory SkyCat tool to visualize the focal plane projected on the sky. The software allows users to load any fits image file with a valid world coordinate system (WCS) or access archival images from the Digital Sky Survey or 2 $\mu$ m All Sky Survey (2MASS) and place slits of user-defined length and width within the field of view of MODS or LUCI. The mask design software for both of these facility instruments have undergone significant upgrades, primarily to fix several known bugs, but also to improve the user mask design experience. Although both software allow users to manually place individual slits on a mask, a more useful feature is the Auto-Slit feature. It is a tool used to automatically place slits on sources in a user provided catalog. While this feature had been present in both LMS and MMS, its functionality was limited to a narrow range of PAs. The recent software updates allow users to now run Auto-Slit at any PA. The user may also prioritize targets in a user supplied catalog when optimizing the placement of slits.

The instrument and mask design requirements differ between MODS and LUCI. As a cryogenic instrument, LUCI has a thermal component to the scaling factor that does not exist for MMS. This LMS scale factor was refined and optimized in the latest upgrade. In addition to critical feature improvements, the user interface, including menus, were reorganized to help guide the users through the mask design process. The software now provides guidelines to users, such as warning users when slits overlap (which would result in dispersed light from

one slit contaminating the dispersed light of another slit), and placing boundary guides to notify users when slits are placed in sub-optimal position on the detector. Overlays and verification checks for each instrument were custom tailored to highlight the instrument mask requirements and recommendations. For example, the image quality for MODS decreases rapidly outside a 5.6' diameter circle, primarily due to a combination of astigmatism from the off-axis parabolic collimator mirrors and off-axis aberrations in the f/15 direct Gregorian focal plane. For LUCI, the slit masks are held in a cylindrical shape to follow the curved telescope focal surface along the Y direction so as you move off the center of the field in X, the slitlets on a MOS mask become increasingly out of focus with respect to both the telescope (giving higher slit losses) and the instrument (decreasing the effective resolution). The overlays and verification checks for each instrument have been tailored to reflect the horizontal IQ dependence for LUCI, and radial distortion for MODS. LMS has the ability to place alignment stars without cut boxes. This ability increases the number of slits that can be placed on a mask, the overall magnitude range of alignment stars, the precision of alignment, as well as our sky coverage with LUCI MOS masks. MODS alignment routines have significantly changed and improved over the years and MMS was upgraded to reflect the alignment box requirements for those alignment routines. Most critically, the latest upgrades are fully backwards compatible. Future improvements will include the ability to directly include AO reference stars for ESM MOS observations into the mask design.

Figure 9 shows an ACS/HST image of the Antennae (NGC 4038/39) loaded into the updated LMS software. The slits are placed on young star clusters identified from a catalog.<sup>22</sup> The image on the right in Figure 8 shows the Gerber mask design which is sent for fabrication with a laser cutting machine located at the University Research Instrumentation Center (URIC) at the University of Arizona (see Reynolds et al. 2014<sup>23</sup>). There is a single deadline each semester for the submission of MODS and LUCI masks to LBTO. The masks are then reviewed by the LBTO Mask Scientist before being fabricated.

MODS and LUCI masks are kept in inventory on the mountain. MOS masks can be reused over the course

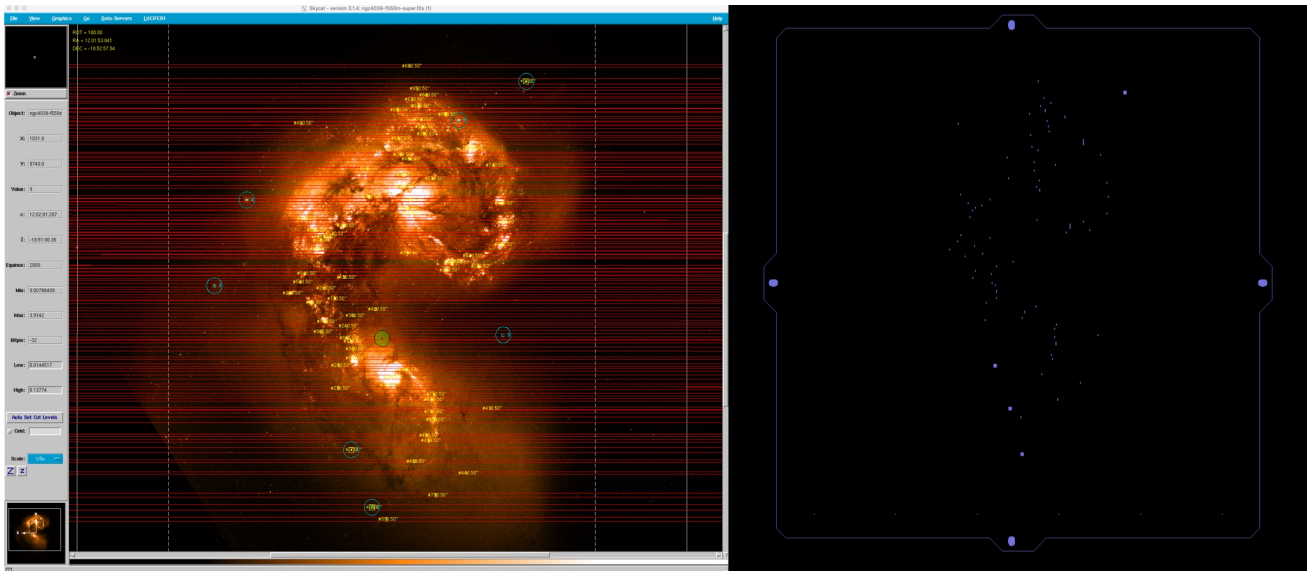


Figure 9: Left - The main GUI for the LUCI LMS software (similar to the MODS MMS GUI). The GUI shows a WCS corrected image from HST of the Antennae with the slits overlaid. Note the square  $2'' \times 2''$  reference boxes used for alignment Right - a gerber (gbr) file showing the location of slits and alignment boxes. This file contains the information (location of boxes and slits) used to manufacture the mask at URIC.

of multiple semesters. With the move to “all-binocular-all-the-time” the standard procedure is to fabricate two copies of MODS MOS masks and up to four copies of LUCI MOS masks (in case the same masks are required for back-to-back mask exchanges). PIs are also free to use different MOS masks (some PAs and pointing center) for the same science field.

### 3.6 Adaptive Optics Observations with LUCI

Unlike many AO systems where the wavefront sensor (WFS) and the deformable mirror (or mirrors) reside on a common optical bench that lies between a focal port and an instrument (or suite of instruments), the LBT uses Adaptive Secondary Mirrors (ASM). The ASMs are designed to operate in either AO mode, or in SL mode by maintaining a fixed flat shape. The ASMs are each mounted on a secondary mirror swing-arm for their respective SX (left) or DX (right) primary mirrors. Each ASM has 672 actuators driving a deformable shell and is used in conjunction with a pyramid wavefront sensor to correct atmospheric turbulence using the flux and observed point-spread function (PSF) of natural guidestars (NGS) also called AO Reference stars. Like the guide-cameras, these AO Reference stars must be selected from a  $2' \times 3'$  patrol field. The N30 FOV lies entirely within the patrol field. Each scientific instrument that is AO-capable houses its own pyramid wavefront sensor system. The first ASM was mounted on the DX side of LBT in May 2010, and the second ASM was installed on the SX side in 2011. The first light AO (FLAO) was not originally commissioned with the LUCIs. Only in 2014 with the installation of the N30 AO cameras was FLAO used with each of the LUCIs. For more detailed information on construction, commissioning, and FLAO operations see Christou et al. (2018),<sup>24</sup> and references therein,

The FLAO system was recently upgraded to the Single conjugated adaptive Optics Upgrade for LBT (SOUL). SOUL commissioning began on LUCI-1 in September 2018 and has continued through the 2020B semester. No further commissioning time is planned for SOUL on SX with LUCI-1. SOUL first light for LUCI-2/DX was December 2019, but a critical failure in the DX ASM forced its removal in spring 2020, putting SOUL DX LUCI-2 commissioning on hiatus. SOUL improvements include: faster loop framerates (up to 2kHz), more modes applied for corrections; sensitivity to fainter AO Reference star, decreasing the limiting magnitude from  $R \simeq 15.5$  to  $R \simeq 18$  (verified on-sky); and improved strelh ratios at fainter limiting magnitudes (Pinna et al. 2016<sup>25</sup>).

The LUCIs can make use of the AO system in three ways. The first is via ARGOS (Advanced Rayleigh guides Ground layer adaptive Optics System) a set of 6 green ( $\lambda = 0.532 \mu\text{m}$ ) lasers (3 per side) used to correct for ground layer atmospheric turbulence. ARGOS requires an NGS for “truth” sensing the low order corrections, particularly tip and tilt. This is because laser guidestars (LGS) provide poor tip and tilt information. Originally, ARGOS had its own NGS wavefront sensor, but due to issues with the system, switched to using FLAO and now SOUL. ARGOS is designed to be used with the N3.75 camera for either imaging or spectroscopic observations, including MOS. The system does not provide diffraction limited observations, but is designed to improve the natural seeing by at least  $2\times$ . First results are described in Rabien et al. 2019.<sup>26</sup> ARGOS has been transitioned to SOUL on SX. However, ARGOS is not currently available for on-sky science observations due to several hardware issues that need to be addressed.

The LUCIs can also use AO via DL and ESM observations. As noted earlier, LUCI DL AO uses the N30 camera with a  $30'' \times 30''$  FOV and is currently limited to imaging only on LUCI-1. DL AO has been available for shared-risk in some capacity since early 2017. Although availability has been limited by various hardware and technical issues. Currently, the SOUL upgrade is available for shared-risk use on LUCI-1.

In November 2020, a SOUL Science Commissioning run was executed over six nights using LUCI-1. The LBTO community were invited and encouraged to submit imaging proposals using diffraction limited (DL) AO. Half of the programs submitted and approved for time were completed during the run. Unfortunately, one-third of the time was lost to weather, and a significant fraction of the time was affected by poor seeing. Figure 10 (left) is a pseudo-color image of Uranus created from  $J$ -,  $H$ -, and  $K$ -band full AO observations obtained during the run.

In addition to full AO corrections, the application a few low-order modes to improve the PSF has been tested on-sky since the first commissioning of FLAO.<sup>27</sup> Those test were able to achieve a strelh ratio  $\simeq 3.5\%$  and a FWHM  $\simeq 0''.24$  with a simulated  $R < 17$  star and 10 modes of corrections applied. Development was continued by LBTO staff in 2014 where this was tested using the N3.75 camera in order to significantly improve the natural seeing over a larger FOV. This was called Enhanced Seeing Mode (ESM) and was finalized to include 11 modes: tip, tilt, focus, 2 astigmatism, 2 coma, 2 trefoil, spherical, and 1 “high” order. ESM uses the same AO reference star patrol field as DL and has the same flux limitations. More systematic testing of ESM using FLAO began in mid-2018 by LBTO staff in an attempt to better quantify its capabilities. These tests included revisiting a set of “standard” fields, obtaining ESM observations in parallel with SL observations to better quantify the improvements over natural seeing conditions. The first results were presented in Rothberg et al. 2018,<sup>2</sup> and showed a significant improvement in the natural seeing. Follow-up work was presented in Rothberg et al. 2019<sup>28</sup>

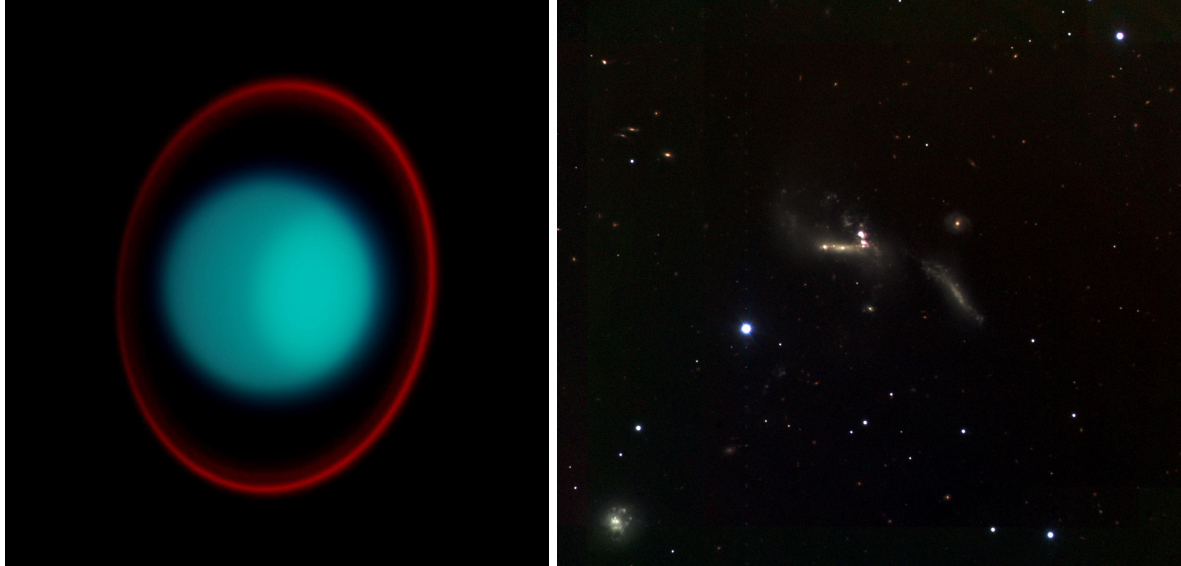


Figure 10: (left) Pseudo-color image of Uranus assembled from  $J$ -band,  $H$ -band, and  $K$ -band AO observations. The observations used 90 modes of correction with a loop frequency of 836 Hz. The total exposure time was 210 seconds at  $J$ -band, 180 seconds at  $H$ -band, and 420 seconds at  $K$ -band. The zenith corrected natural seeing at 0.5m, as measured by the differential image motion monitor (DIMM), was  $0''.7$ - $0''.8$  during the observations. The FWHM as measured from the AO Reference “star” Ariel was  $0''.14$ ,  $0''.11$ , and  $0''.1$  at  $J$ ,  $H$ , and  $K$ -band, respectively. (right) Pseudo-color image of Hickson Compact Group 31 assembled from  $J$ -band,  $H$ -band, and  $K$ -band observations using the Enhanced Seeing Mode. This mode uses the N3.75 camera with 11 modes of correction. The DIMM seeing was  $0''.6$ - $0''.7$ . The measured FWHM was  $0''.5$  at  $J$ -band,  $0''.42$  at  $H$ -band, and  $0''.32$  at  $K$ -band. The observations were taken with 2-3 magnitudes of extinction from clouds. The total exposure time was 10 minutes at  $J$ -band and 18 minutes at both  $H$ - and  $K$ -band.

demonstrated that in the best natural seeing conditions a FWHM  $\simeq 0''.22$  could be routinely achieved. In poor conditions (natural seeing approaching  $2''$ ) improvements as large as  $3\times$  were seen at  $K$ -band and  $\simeq 2\times$  at  $J$ -band. ESM has become a dual system: capable of achieving near-Hubble PSFs, but over a FOV twice in size using imaging or spectroscopy (including MOS masks); or a system that can be used to “rescue” nights with poor conditions that would otherwise be lost and achieving average seeing conditions. Since the upgrade to SOUL on SX, characterization of ESM capabilities has continued, and preliminary results will be presented in a companion SPIE paper. Figure 10 (right) shows a pseudo-color ( $J$ ,  $H$ , and  $K$ ) image obtained with SOUL and ESM using LUCI-1 of the Hickson Compact Group 31. While observations were taken during cloudy conditions, the observations were able to achieve a FWHM  $\simeq 0''.3$  at  $K$ -band.

### 3.7 Potsdam Echelle Polarimetric and Spectroscopic Instrument (PEPSI)

PEPSI is an optical high-resolution ( $50,000 < R < 250,000$ ) fiber-fed echelle spectrograph. It is fed through either the bent  $f/15$  Gregorian foci on SX and DX, or through polarimeters attached to the direct Gregorian  $f/15$  port behind the primary mirrors. The latter requires the removal of the MODS instruments. The bent Gregorian foci contain a permanent fiber unit (PFU) which feeds non-polarized on-axis and off-axis light via a fiber-train to the spectrograph which is mounted below the pier of the telescope (see Figure 1). Each focal station contains three fiber sizes which determine the spectral resolution achieved. Regardless of fiber size or resolution, PEPSI observations of non-polarized light can cover the range of  $0.384 < \lambda < 0.913 \mu\text{m}$ . Continuous wavelength coverage is achieved through three exposures and six cross dispersers. The polarimeters are able to measure the four Stokes IQUV parameters. PEPSI has been used on sky since late 2015 and the polarimeters saw first light on September 11, 2017. Currently, a two week polarimetric campaign is being conducted at LBTO. Figure 11 summarizes the various PEPSI user modes. For more information, see Strassmeier et al. (2008)<sup>29</sup> and (2015).<sup>29</sup>

PEPSI has been successfully used in “mixed-mode” configurations. During two recent LBTI campaigns, the

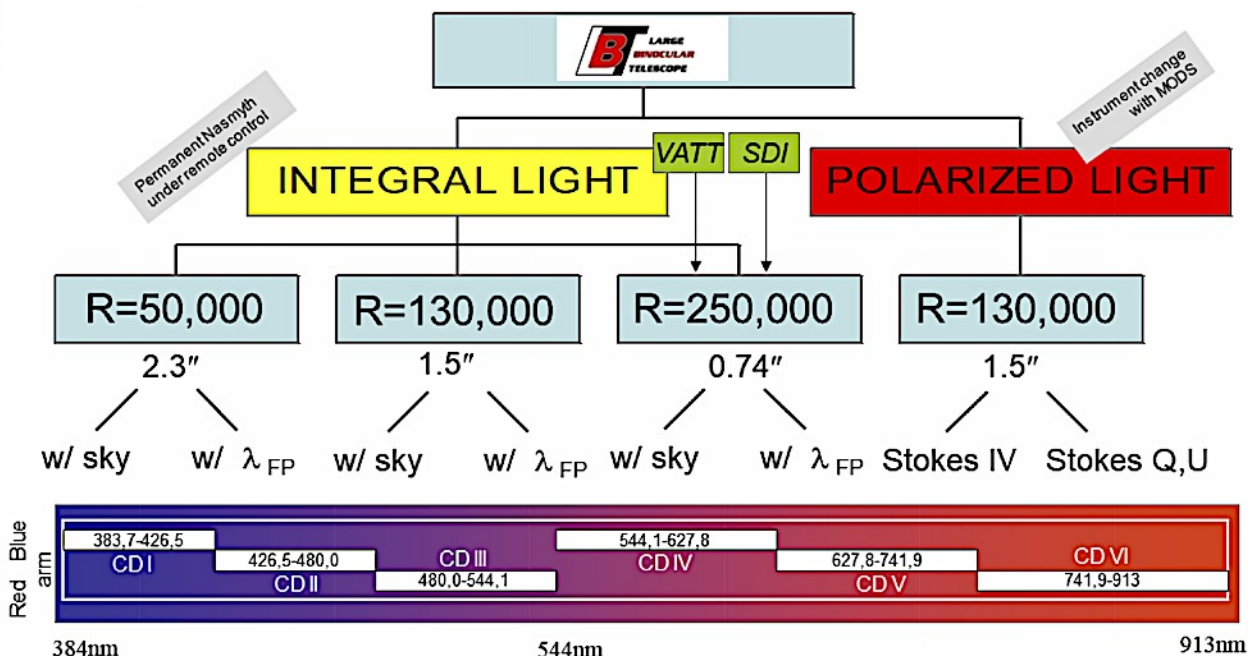


Figure 11: Overview of the potential PEPSI configurations available to the LBTO community,

LBTI instruments were used on SX while PEPSI was run on the DX side of the telescope. Successful closed dome tests have been made using a combination of PEPSI & MODS and PEPSI with LUCI. PEPSI can also be used independently of the LBT primary mirrors. A 450 meter long fiber connection is installed between the VATT and the PEPSI spectrograph, allowing for observations independently of LBT. PEPSI is also used during the daytime to obtain continual observations of the Sun using the robotic solar-disk-integration (SDI) telescope. This is a 1 cm telescope installed on the lanai of the LBT enclosure on the second floor.

As noted earlier, PEPSI was originally a PI instrument. It was decided by the LBT board that PEPSI should begin the transition from PI instrument to facility instrument during 2020. Part of the transition included the installation of PEPSI data processing computers on the summit, training LBTO staff to operate the instrument, with the goal of making the instrument available for use any night in the same way as the other three facility instruments. However, the timetable for completion of this transfer has been altered by the ongoing COVID-19 pandemic. Staff training is proceeding slowly, with service observers and staff astronomers eavesdropping during night observations. Proposals to use PEPSI no longer require approval and collaboration with the instrument PI. However, requests to use PEPSI during partner science time requires arrangements to be made well in advance of the requested nights. This is to allow AIP staff time to coordinate and execute the observations at night.

#### 4. HEALTH AND INSTRUMENT PERFORMANCE PLAN FOR THE OBSERVATORY (HIPO)

This project will develop a system which monitors the health and performance of the three pairs of facility instruments: LBCs, MODS, and LUCIs. Although our partner science observers interact with the instruments on a nightly basis, they may not have the same experience or knowledge to discern anything but the most serious problems. Further, data may not be analyzed by partner science teams until some time after collection. Thus, relying on visiting observers to notify the observatory of potential issues may result in a significant delay before they can be addressed, or, result in spending time chasing false leads. Early and quick detection of problems will reduce the downtime and impact to partner science operations and reduce the potential for recurring, long-term and/or permanent damage to the instruments. The project aims to automate some or all of the monitoring of

instruments where and when possible. The science and engineering operations groups would be notified of any potential anomalies or unusual behavior as quickly as possible and work with mountain staff to quickly address any issues. HIPO includes development of software, or integration of already existing packages, to process and analyze data collected during day and night activities. It will also include regular observations of calibration data (closed dome) and on-sky instrument calibrations (such as zeropoints) to detect any loss of sensitivity as early as possible. These data would be made available online to review the previous night’s status of an instrument as well as allow for short and long-term monitoring. A project plan for HIPO has already been approved, and work on calibration data has been underway. Given the recent changes in observatory operations, HIPO has progressed somewhat slower than originally projected. However, because LBTO staff are now operating the facility instruments on a nightly basis, trained staff are able to quickly address issues should they arise.

## 5. ALL BINOCULAR ALL THE TIME

LBT was designed to operate in binocular mode on-sky. Since late 2017, all three facility instruments have been installed and commissioned (although not all modes released) and thus capable of operating in binocular configurations. Table 2 below shows the binocular operating status of each of the facility instruments in 2018 and 2019. Data are scraped from night reports and reported downtimes.

| LBC | None | Mono  | Bino  | MODS | None | Mono  | Bino  | LUCI | None | Mono  | Bino  |
|-----|------|-------|-------|------|------|-------|-------|------|------|-------|-------|
| 19B | 0%   | 3.3%  | 96.7% | 19B  | 0%   | 1.3%  | 98.7% | 19B  | 2.6% | 23.2% | 74.2% |
| 19A | 0%   | 0%    | 100%  | 19A  | 0%   | 2%    | 98%   | 19A  | 1.3% | 22.5% | 76.3% |
| 18B | 0%   | 0%    | 100%  | 18B  | 2.2% | 6%    | 91.8% | 18B  | 2%   | 5.3%  | 92.8% |
| 18A | 0%   | 11.2% | 88.8% | 18A  | 0.7% | 11.9% | 87.3% | 18A  | 0.7% | 12.9% | 86.3% |

Table 2: Instrument Availability of LBC, MODS, and LUCI during 2018-2019.

## ACKNOWLEDGMENTS

B. Rothberg would like to thank R.T. Gatto for useful discussions and providing much needed support for the work presented here.

## REFERENCES

- [1] Rothberg, B., Kuhn, O., Edwards, M. L., Hill, J. M., Thompson, D., Veillet, C., and Wagner, R. M., “Current status of the facility instrumentation suite at the Large Binocular Telescope Observatory,” in [*Ground-based and Airborne Telescopes VI*], *Proc. SPIE* **9906**, 990622 (July 2016).
- [2] Rothberg, B., Kuhn, O., Power, J., Hill, J. M., Veillet, C., Edwards, M., Thompson, D., and Wagner, R. M., “Current status of the facility instruments at the Large Binocular Telescope Observatory,” in [*Ground-based and Airborne Instrumentation for Astronomy VII*], Evans, C. J., Simard, L., and Takami, H., eds., *Society of Photo-Optical Instrumentation Engineers (SPIE) Conference Series* **10702**, 1070205 (July 2018).
- [3] Stone, J. M., Skemer, A. J., Hinz, P., Briesemeister, Z., Barman, T., Woodward, C. E., Skrutskie, M., and Leisenring, J., “On-sky operations with the ALES integral field spectrograph,” in [*Ground-based and Airborne Instrumentation for Astronomy VII*], Evans, C. J., Simard, L., and Takami, H., eds., *Society of Photo-Optical Instrumentation Engineers (SPIE) Conference Series* **10702**, 107023F (July 2018).
- [4] Leisenring, J. M., Skrutskie, M. F., Hinz, P. M., Skemer, A., Bailey, V., Eisner, J., Garnavich, P., Hoffmann, W. F., Jones, T., Kenworthy, M., Kuzmenko, P., Meyer, M., Nelson, M., Rodigas, T. J., Wilson, J. C., and Vaitheeswaran, V., “On-sky operations and performance of LMIRcam at the Large Binocular Telescope,” in [*Ground-based and Airborne Instrumentation for Astronomy IV*], *Proc. SPIE* **8446**, 84464F (Sept. 2012).

- [5] Hoffmann, W. F., Hinz, P. M., Defrère, D., Leisenring, J. M., Skemer, A. J., Arbo, P. A., Montoya, M., and Mennesson, B., “Operation and performance of the mid-infrared camera, NOMIC, on the Large Binocular Telescope,” in [*Ground-based and Airborne Instrumentation for Astronomy V*], *Proc. SPIE* **9147**, 91471O (July 2014).
- [6] Spalding, E., Hinz, P., Morzinski, K., Ertel, S., Grenz, P., Maier, E., Stone, J., and Vaz, A., “Status of commissioning stabilized infrared Fizeau interferometry with LBTI,” in [*Society of Photo-Optical Instrumentation Engineers (SPIE) Conference Series*], *Society of Photo-Optical Instrumentation Engineers (SPIE) Conference Series* **11117**, 111171S (Sept. 2019).
- [7] Herbst, T. M., Santhakumari, K. K. R., Klettke, M., Arcidiacono, C., Bergomi, M., Bertram, T., Berwein, J., Bizenberger, P., Briegel, F., Farinato, J., Marafatto, L., Mathar, R., McGurk, R., Ragazzoni, R., and Viotto, V., “Commissioning multi-conjugate adaptive optics with LINC-NIRVANA on LBT,” in [*Adaptive Optics Systems VI*], Close, L. M., Schreiber, L., and Schmidt, D., eds., *Society of Photo-Optical Instrumentation Engineers (SPIE) Conference Series* **10703**, 107030B (July 2018).
- [8] De La Peña, M. D., Terrett, D. L., Thompson, D., and Biddick, C. J., “Practical considerations for pointing a binocular telescope,” in [*Software and Cyberinfrastructure for Astronomy*], *Proc. SPIE* **7740**, 77402F (July 2010).
- [9] Hill, J. M., Ragazzoni, R., Baruffolo, A., Biddick, C. J., Kuhn, O. P., Diolaiti, E., Thompson, D., and Rakich, A., “Prime focus active optics with the Large Binocular Telescope,” in [*Ground-based and Airborne Telescopes II*], *Proc. SPIE* **7012**, 70121M (July 2008).
- [10] Stangalini, M., Hill, J. M., Pedichini, F., Giallongo, Baruffolo, A., Ragazzoni, R., and Fontana, A., “Technical Report: LBC Wavefront Reconstructio Software upgrade,” tech. rep., INAF-OAR National Institute for Astrophysics (Apr. 2014).
- [11] Rakich, A., Schurter, P., Conan, R., Hill, J. M., Gardiner, M., Bec, M., and Kuhn, O., “Prototyping the GMT telescope metrology system on LBT,” in [*Ground-based and Airborne Telescopes VII*], Marshall, H. K. and Spyromilio, J., eds., *Society of Photo-Optical Instrumentation Engineers (SPIE) Conference Series* **10700**, 107001S (July 2018).
- [12] Rodriguez, S., Rakich, A., Hill, J., Kuhn, O., Brendel, T., Veillet, C., Kim, D. W., and Choi, H., “Implementation of a laser-truss based telescope metrology system at the Large Binocular Telescope,” in [*Optical Manufacturing and Testing XIII*], Kim, D. W. and Rascher, R., eds., **11487**, 78 – 87, International Society for Optics and Photonics, SPIE (2020).
- [13] Pogge, R. W., Atwood, B., O’Brien, T. P., Byard, P. L., Derwent, M. A., Gonzalez, R., Martini, P., Mason, J. A., Osmer, P. S., Pappalardo, D. P., Zhelem, R., Stoll, R. A., Steinbrecher, D. P., Brewer, D. F., Colarosa, C., and Teiga, E. J., “On-sky performance of the Multi-Object Double Spectrograph for the Large Binocular Telescope,” in [*Ground-based and Airborne Instrumentation for Astronomy IV*], *Proc. SPIE* **8446**, 84460G (Sept. 2012).
- [14] Marshall, J. L., O’Brien, T. P., Atwood, B., Byard, P. L., DePoy, D. L., Derwent, M., Eastman, J. D., Gonzalez, R., Pappalardo, D. P., and Pogge, R. W., “An image motion compensation system for the multi-object double spectrograph,” in [*Society of Photo-Optical Instrumentation Engineers (SPIE) Conference Series*], *Proc. SPIE* **6269**, 62691J (June 2006).
- [15] Rothberg, B., Kuhn, O., Veillet, C., and Allanson, S., “GRB 200826A,” *GRB Coordinates Network* **28319**, 1 (Aug. 2020).
- [16] Rossi, A., D’Avanzo, P., D’Elia, V., Melandri, A., Palazzi, E., Rothberg, B., Kuhn, O., and Veillet, C., “GRB 200826A,” *GRB Coordinates Network* **28949**, 1 (Nov. 2020).
- [17] Svinkin, D., Frederiks, D., Ridnaia, A., Tsvetkova, A., and Konus-Wind Team, “GRB 200826A: further analysis of the Konus-Wind data and classification,” *GRB Coordinates Network* **28301**, 1 (Aug. 2020).
- [18] Seifert, W., Appenzeller, I., Baumeister, H., Bizenberger, P., Bomans, D., Dettmar, R.-J., Grimm, B., Herbst, T., Hofmann, R., Juette, M., Laun, W., Lehmitz, M., Lemke, R., Lenzen, R., Mandel, H., Polsterer, K., Rohloff, R.-R., Schuetze, A., Seltmann, A., Thatte, N. A., Weiser, P., and Xu, W., “LUCIFER: a Multi-Mode NIR Instrument for the LBT,” in [*Instrument Design and Performance for Optical/Infrared Ground-based Telescopes*], Iye, M. and Moorwood, A. F. M., eds., *Proc. SPIE* **4841**, 962–973 (Mar. 2003).

- [19] Buschkamp, P., Hofmann, R., Gemperlein, H., Polsterer, K., Ageorges, N., Eisenhauer, F., Lederer, R., Honsberg, M., Haug, M., Eibl, J., Seifert, W., and Genzel, R., “The LUCIFER MOS: a full cryogenic mask handling unit for a near-infrared multi-object spectrograph,” in [*Ground-based and Airborne Instrumentation for Astronomy III*], *Proc. SPIE* **7735**, 773579 (July 2010).
- [20] Pramskiy, A., Thompson, D., Heidt, J., Seifert, W., Gredel, R., and Quirrenbach, A., “The LUCI@LBT twins: instrument flexure control,” in [*Ground-based and Airborne Instrumentation for Astronomy VII*], Evans, C. J., Simard, L., and Takami, H., eds., *Society of Photo-Optical Instrumentation Engineers (SPIE) Conference Series* **10702**, 107022X (July 2018).
- [21] Pfeifle, R. W., Satyapal, S., Manzano-King, C., Cann, J., Sexton, R. O., Rothberg, B., Canalizo, G., Ricci, C., Blecha, L., Ellison, S. L., Gliozzi, M., Secrest, N. J., Constantin, A., and Harvey, J. B., “A Triple AGN in a Mid-infrared Selected Late-stage Galaxy Merger,” **883**, 167 (Oct. 2019).
- [22] Whitmore, B. C., Chandar, R., Schweizer, F., Rothberg, B., Leitherer, C., Rieke, M., Rieke, G., Blair, W. P., Mengel, S., and Alonso-Herrero, A., “The Antennae Galaxies (NGC 4038/4039) Revisited: Advanced Camera for Surveys and NICMOS Observations of a Prototypical Merger,” *The Astronomical Journal* **140**, 75–109 (July 2010).
- [23] Reynolds, R. O., Derwent, M., Power, J., Kuhn, O., Thompson, D., O’Brien, T. P., Pogge, R. W., and Wagner, R. M., “The instrument focal plane mask program at the Large Binocular Telescope,” in [*Advances in Optical and Mechanical Technologies for Telescopes and Instrumentation*], *Proc. SPIE* **9151**, 91514B (July 2014).
- [24] Christou, J. C., Brusa, G., Conrad, A., Hill, J., Miller, D. L., Rahmer, G., Taylor, G. E., Veillet, C., and Zhang, X., “Adaptive optics systems at the Large Binocular Telescope: status, upgrades, and improvements,” in [*Adaptive Optics Systems VI*], Close, L. M., Schreiber, L., and Schmidt, D., eds., *Society of Photo-Optical Instrumentation Engineers (SPIE) Conference Series* **10703**, 107030A (July 2018).
- [25] Pinna, E., Esposito, S., Hinz, P., Agapito, G., Bonaglia, M., Puglisi, A., Xompero, M., Riccardi, A., Briguglio, R., Arcidiacono, C., Carbonaro, L., Fini, L., Montoya, M., and Durney, O., “SOUL: the Single conjugated adaptive Optics Upgrade for LBT,” in [*Adaptive Optics Systems V*], *Proc. SPIE* **9909**, 99093V (July 2016).
- [26] Rabien, S., Angel, R., Barl, L., Beckmann, U., Busoni, L., Belli, S., Bonaglia, M., Borelli, J., Brynnel, J., Buschkamp, P., Cardwell, A., Contursi, A., Connot, C., Davies, R., Deysenroth, M., Durney, O., Eisenhauer, F., Elberich, M., Esposito, S., Frye, B., Gaessler, W., Gasho, V., Gemperlein, H., Genzel, R., Georgiev, I. Y., Green, R., Hart, M., Kohlmann, C., Kulas, M., Lefebvre, M., Mazzoni, T., Noenickx, J., Orban de Xivry, G., Ott, T., Peter, D., Puglisi, A., Qin, Y., Quirrenbach, A., Raab, W., Rademacher, M., Rahmer, G., Rosensteiner, M., Rix, H. W., Salinari, P., Schwab, C., Sivitilli, A., Steinmetz, M., Storm, J., Veillet, C., Weigelt, G., and Ziegler, J., “ARGOS at the LBT. Binocular laser guided ground-layer adaptive optics,” **621**, A4 (Jan. 2019).
- [27] Esposito, S., Riccardi, A., Pinna, E., Puglisi, A., Quirós-Pacheco, F., Arcidiacono, C., Xompero, M., Briguglio, R., Agapito, G., Busoni, L., Fini, L., Argomedo, J., Gherardi, A., Brusa, G., Miller, D., Guerra, J. C., Stefanini, P., and Salinari, P., “Large Binocular Telescope Adaptive Optics System: new achievements and perspectives in adaptive optics,” in [*Astronomical Adaptive Optics Systems and Applications IV*], Tyson, R. K. and Hart, M., eds., *Society of Photo-Optical Instrumentation Engineers (SPIE) Conference Series* **8149**, 814902 (Oct. 2011).
- [28] Rothberg, B., Christou, J. C., Miller, D. L., Thompson, D., Taylor, G. E., and Veillet, C., “Enhanced Seeing Mode at the LBT: A Method to Significantly Improve Angular Resolution over a 4' x 4' Field of View,” *arXiv e-prints*, arXiv:1911.00549 (Nov. 2019).
- [29] Strassmeier, K. G., Ilyin, I., Järvinen, A., Weber, M., Woche, M., Barnes, S. I., Bauer, S. M., Beckert, E., Bittner, W., Bredthauer, R., Carroll, T. A., Denker, C., Dionies, F., DiVarano, I., Döscher, D., Fechner, T., Feuerstein, D., Granzer, T., Hahn, T., Harnisch, G., Hofmann, A., Lesser, M., Paschke, J., Pankratow, S., Plank, V., Plüschke, D., Popow, E., and Sablowski, D., “PEPSI: The high-resolution échelle spectrograph and polarimeter for the Large Binocular Telescope,” *Astronomische Nachrichten* **336**, 324 (May 2015).